Icarus 390 (2023) 115303

Contents lists available at ScienceDirect

Icarus

journal homepage: www.elsevier.com/locate/icarus

Letter

Supervolcanic resurfacing in northwestern Arabia Terra, Mars

Augustus Bates [a,*], S. Goossens [b], J.M. Lorenzo [a], L. Ojha [c], D.R. Hood [d], S. Karunatillake [a], S. Kobs Nawotniak [e], T. Paladino [e]

[a] Department of Geology and Geophysics, Louisiana State University, Baton Rouge, LA, USA
[b] NASA Goddard Space Flight Center
[c] Rutgers, The State University of New Jersey
[d] Baylor University
[e] Idaho State University

ARTICLE INFO

Keywords:
Volcanism
Mars
Geochemistry
Supereruptions
Remote sensing

ABSTRACT

An area roughly 9 × 10^5 km^2 within northwest Arabia Terra contains several depressions interpreted to be supervolcanic calderas, contained within a chemical province considered consistent with large-scale igneous processes. Despite the underlying global significance to climate and geology, the supervolcanic hypothesis is yet to be tested with comprehensive compositional or geophysical analyses. Here we present geochemical evidence consistent with regional-scale supervolcanic resurfacing, with associated eruptions capable of degassing a climate-altering ~10^8 kg of sulfur phases. Through gravitational modeling, we find evidence of low-density pyroclastic loading within this region, and a low elastic thickness, suggestive of a higher heat flow during the eruptive process. Our geochemical observations within this region reinforce its compositional uniqueness compared to contemporaneous volcanoes.

1. Introduction

Through near global sampling of martian surface geochemistry, six chemically distinct provinces were derived some of which correlated to major volcanic provinces or were interpreted to retain chemical signatures dating to their respective times of emplacement (Taylor et al., 2010). Chemical province 6 (Fig. 1) which exists in and near Arabia Terra, is unique among the others as it is enriched in all elements measured by gamma ray spectroscopy (GRS), but its origin remains ambiguous (Karunatillake et al., 2009; Taylor et al., 2010). These elemental trends could indicate igneous activity, especially when considering the abundance of friable material within Arabia Terra (Bandfield et al., 2013; Michalski and Bleacher, 2013). In fact, Michalski and Bleacher (2013) identified four possible volcanic sources that could explain this chemistry. The individual eruption volumes from these paterae could have been in excess of 4600 km^3, much larger than the threshold (1000 km^3) required to classify an eruption as a supereruption (Baines and Sparks, 2005). Supereruptions are a viable mechanism to explain both the chemistry of chemical province 6 and the abundance of friable material within Arabia. There have been further attempts to establish the presence of such eruptions within Arabia (Whelley et al., 2021), but none have examined the regional chemistry in context with other volcanic or sedimentary regions on Mars. Here, we explain the origin of chemical province 6's chemistry within Arabia through supervolcanism. We find that the notable enrichments in volatile species, radiogenic elements, and Si when compared to the average martian crust are most consistent with a supervolcanic provenance.

In this study, we attempt to resolve the provenance of the chemistry of the supervolcanic context region (SCR). SCR is defined as the highlands region which contains the paterae and consists only of chemical province 6 (Taylor et al., 2010) (Fig. 1). SCR is meant to represent the regional chemistry that is distinct from the surrounding Arabia Terra according to Taylor et al. (2010) and that also overlaps with the four candidate calderas as outlined by Michalski and Bleacher (2013) (Fig. 1). SCR is surrounded by a broader region (broad SCR or BSCR), which contains rock units that date to the Early, Middle and Late Noachian and whose outermost boundaries are defined by a change in elevation (Carnes et al., 2017). We treat SCR as distinct from BSCR without overlapping chemical map pixels so as to better examine the chemical differences between the two. In general, the regional chemistry of SCR exhibits enrichments in all elements measured by GRS (Supplementary Information, Fig. S2). Prior works suggest that this chemistry

* Corresponding author.
E-mail address: abate15@lsu.edu (A. Bates).

https://doi.org/10.1016/j.icarus.2022.115303
Received 22 March 2022; Received in revised form 3 October 2022; Accepted 4 October 2022
Available online 11 October 2022

could be from volcanic activity due to enrichments in Fe, K and Th (Michalski and Bleacher, 2013; Taylor et al., 2010). Alternatively, SCR's associated chemical trends relative to the Martian crust, especially H_2O enrichment, can support the interpretation that the region holds a massive sedimentary basin (Dohm et al., 2007). Because the lack of other spectral chemical data could result from dust accumulation (Newsom et al., 2007) we propose to uncover the provenance of SCR's chemistry by considering spatial abundance trends in chemical pairs K and Th, S and Cl primarily within SCR.

In addition, we conduct a gravitational admittance analysis of SCR (Fig. 3A) to constrain the load density, porosity, and elastic thickness of the region. Load density estimations inform us of the relative composition of the material which is present in SCR. Due to the relatively small variations in topography within Arabia, our estimations of load density from admittance are best considered as upper-crust densities. Our estimations of elastic thickness can be used to bound the range of possible regional heat flow values. We use elastic thickness estimates as proxies for regional heat flow (McGovern et al., 2004), which has implications for SCR's inferred eruptive regime.

2. Data and methods

We examine the chemistry of SCR using GRS-derived chemical data because they are ideal for investigating regional trends in the bulk regolith, due to consistent decimeter scale sampling depths for all mapped elements. Their sampling depth is in part due to derivation from averaging across different gamma spectral peaks (Taylor et al., 2010; Viviano et al., 2019) and because of the coarse spatial resolution throughout much of the mid-to-low latitudes (about 60^o to -60^o), with each pixel covering roughly 450 km (Boynton et al., 2007; Hood et al., 2016).

For our geochemical analyses, we emphasize regional K—Th and S—Cl concentration trends because these four elements can effectively discriminate between geologic processes such as volcanism (Baratoux et al., 2011), subaqueous deposition and subaqueous alteration (Ehlmann et al., 2011; Taylor et al., 2006), or dust accumulation that reduces spectral responses (Ojha et al., 2018). For example, K and Th are known to correlate strongly in igneous rocks as incompatible trace elements, in part due to their incompatibility with cation sites in mafic to ultramafic silicates (Taylor et al., 2006). K and Th fractionation trends can also grant insight into prevalence of aqueous alteration of bedrock in a region (Karunatillake et al., 2006; Sawyer et al., 2000; Taylor et al., 2006, 2010). K, as a large ion lithophile, is highly mobile in solution, which contrasts with Th, a much less mobile element due to its high atomic charge (Albarede, 2009). Therefore, in regions which have been subjected to high degrees of aqueous alteration, significant fractionation of K from Th would occur, resulting in a K/Th ratio that is lower than the martian global average (Taylor et al., 2006). We use such trends to investigate if aqueous alteration is a dominant process within SCR, a trend that would arise if NW Arabia functioned as a sedimentary basin or floodplain, suggested by previous studies (Dohm et al., 2007; Kerber et al., 2012; Tanaka, 2000).

We also characterize S and Cl abundance within NW Arabia and compare them to other regions (Fig. 1) to investigate whether their provenance is most consistent with dust accumulation or volcanic degassing. S and Cl are notable volatile constituents in terrestrial volcanic eruptions and share a similar function on Mars (Diez et al., 2009; Keller et al., 2006; Gaillard and Scaillet, 2009; Ojha et al., 2018). As

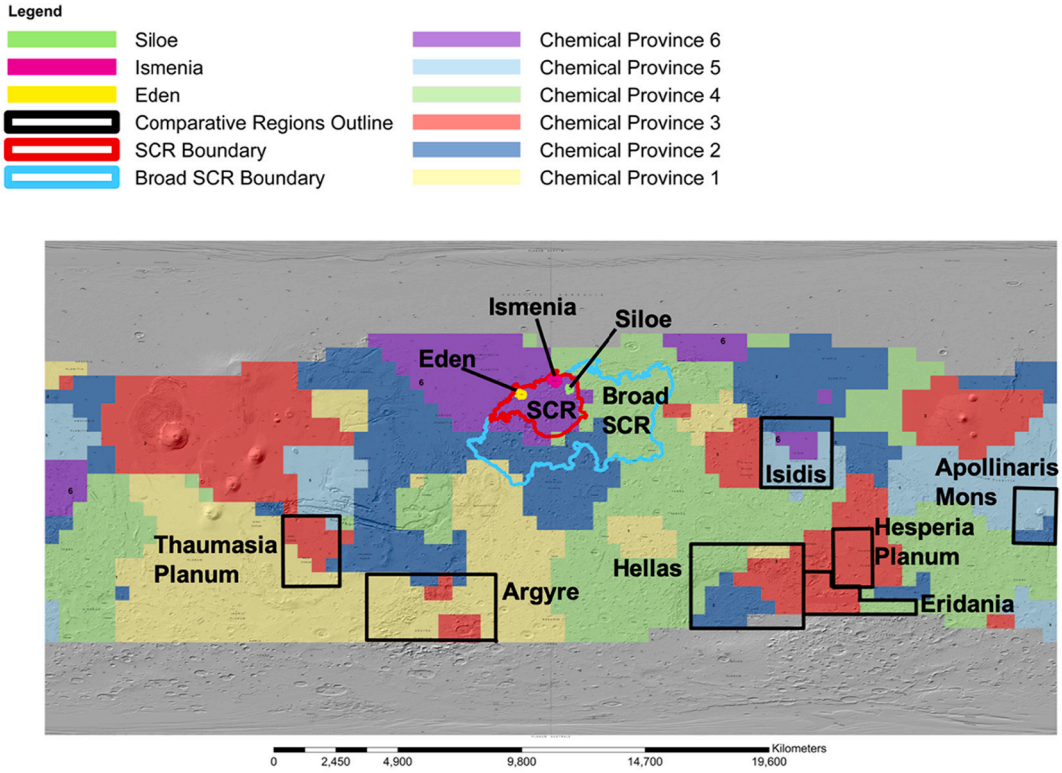

Fig. 1. Geochemical provinces (Taylor et al., 2010) overlain on a topographic map of Mars. SCR and BSCR derived by us are shown along with three previously proposed calderas (Siloe, Ismenia, and Eden) by (Michalski and Bleacher, 2013). SCR is meant to represent the regional chemistry that is distinct from the surrounding Arabia Terra and that also overlaps with the four candidate calderas as outlined by Michalski and Bleacher (2013). SCR is surrounded by BSCR whose outermost boundaries are defined by a change in elevation, and contains rock units that date to the Early, Middle and Late Noachian (Carnes et al., 2017). The black boxes outline comparative regions for compositional study. Our basin references are Argyre, Hellas and Isidis. Our volcanic reference regions are Thaumasia and Hesperia Planae and Apollinaris Mons. We also selected a region to the east of Hellas (Eridania) which is composed of heavily eroded fluvial and volcanic material. More details on region selection can be found in the Supplement.

such, they can serve as a proxy for eruptive explosivity, and offer subtle insight into mantle pressure and temperature regimes (Burton et al., 2009; Edmonds and Wallace, 2017; Ojha et al., 2018; Spilliaert et al., 2006). However, S and Cl are among the most mobile elements on the Martian surface, prone to remobilization through episodic events, such as aqueous alteration processes and atmospheric circulation (King and McLennan, 2010), making compelling arguments into their origins difficult. S and Cl have also been used to characterize a global dust reservoir for Mars, through their consistent molar ratio observed within heavily mantled locales (Ojha et al., 2018).

In addition to our analysis of the regional geochemistry, we attempt to estimate the ranges of average density of the lithosphere within the SCR to assess whether or not the materials there are consistent with a pyroclastic origin. The density of pyroclastic material on Mars is generally around 1500–1900 kg m^{-3} (Ojha and Lewis, 2018), whereas average martian crust density is in general significantly higher, around 2200–2800 kg m^{-3} (Goossens et al., 2017), with some estimates as high as 3200–3400 kg m^{-3} (Baratoux et al., 2014). More recently, it has been found that the density of the martian crust is between 2850 and 3100 kg m^{-3} (Wieczorek et al., 2022). Higher density estimates reflect a crustal origination from primary igneous material, mostly from extensive effusive flows to preserve a low crustal porosity (Baratoux et al., 2014). Lower densities are generally indicative of more friable and porous materials, such as pyroclastic deposits (Ojha and Lewis, 2018). Furthermore, volcanism usually correlates with a higher heat flow, which can be reflected in the elastic thickness of a region. Elastic thickness describes the effective thickness of the deformable lithosphere – a proxy for heat flow and lithosphere-mantle coupling. As such, elastic thickness can offer insight into the thermal environment of a region (Belleguic et al., 2005; Grott and Wieczorek, 2012; McGovern et al., 2002).

Our investigations of regional geochemistry involve comparative analysis between SCR and other geologically unique regions on Mars. We consider specific regions that are geographically distributed for chemical comparisons (Fig. 1). Based on the derived SCR age (Supplementary Information, Fig. S1), we identify three contemporaneous Noachian volcanic provinces as type references for compositional comparisons: Thaumasia Planum, Hesperia Planum, and Apollinaris Mons. Our three igneous references also cover a wide range of eruptive styles, as Apollinaris is inferred to have erupted explosively in its past (Kerber and Head, 2010) whereas Hesperia and Thaumasia are large igneous provinces which produced effusive lava flows (Hood et al., 2016; Tanaka et al., 2014). We also selected several sedimentary references (Hellas, Argyre and Eridania Planitia) that have similar ages as SCR. Our comparative region selections maximize insight from diverse subaerial sedimentary and igneous processes and minimize bias from chemical overprinting across proximal regions (Table 1). Details of the geologic history and chemical interpretation of each region can be found in the supplement. Our comparative regions are delineated following the topography and mapped geology (Tanaka et al., 2014) associated with each comparative region.

3. Results

Of all the regions analyzed in this study, only Apollinaris Mons, Isidis, SCR and BSCR have K/Th ratios that are lower than the crustal average (Table 1). Of these regions, SCR and BSCR have low dispersions of K and Th values whereas Apollinaris and Isidis have large dispersion in their values (Fig. 2A). Individual K abundances for Isidis span from some of the lowest observed in this study to the highest. It is unlikely that areal extent is responsible for this, because Isidis and Apollinaris have a similar areal extent (Table 1), making it more likely that the observed dispersion of K and Th is underpinned by geologic processes. For example, Apollinaris' long active lifetime (Robbins et al., 2011) would maximize the potential for individual eruptions to exhibit chemical heterogeneity to each other. SCR's much lower dispersion in overall K and Th abundances, and a K/Th similar to the crustal average, in comparison to similarly enriched regions, are suggestive of a region not substantially more altered than the whole of the martian surface.

Regions which have a K/Th higher than the crustal average include Argyre, Hellas, Eridania, Thaumasia and Hesperia Planae (Fig. 2A). A high K/Th is generally indicative of aqueous alteration on Mars (Taylor

Table 1
Average chemistry for each martian reference region, spatial extent in chemical map pixels, and geologic analog context for which they served as a reference. Underlying chemical data are the same as used in Figs. 1 and 2. Values for SCR, BSCR and the martian crust are also given. The crustal proxy has SCR and BSCR removed to reduce sampling bias. Overall, our reference regions are close temporal counterparts to SCR. The mean mass fraction for K, Th, S and Cl is given for all the regions with K and Th reported in mg/kg and S and Cl reported as percentages (wt%). The ratios for K/Th and S/Cl are calculated from reported elemental weight percent. The 1 sigma error is the standard error of the mean; ratio error is calculated by $(K/Th)[(\sigma_K/K)^2 + (\sigma_{Th}/Th)^2]^{1/2}$, where K and Th are the mean concentration of K, Th. The same applies to S and Cl.

Region Name	Geologic Analog	Age (Ga)	Average Elemental Abundance (K/Th in mg/kg, S & Cl in wt%) (1σ error)											
			K	Error	Th	Error	K/Th	Error	S	Error	Cl	Error	S/Cl	Error
Hellas (48 pixels)	Impact formed, sedimentary basin	~ 4.1	3007	± 145.2	0.41	± 0.06	7325	± 1138	2.1	± 0.3	0.4	± 0.04	5.1	± 0.8
Argyre (41 pixels)	Impact formed, sedimentary basin	~ 4.0	3021.6	± 107.8	0.49	± 0.04	6144.9	± 601	1.9	± 0.2	0.38	± 0.03	5.0	± 0.7
Isidis (25 pixels)	Impact induced magmatism	~ 3.9–3.8	3860.4	± 120.6	0.69	± 0.05	5625	± 477	1.9	± 0.2	0.49	± 0.03	3.9	± 0.5
Eridania (14 pixels)	Heavily weathered fine-grained material (multiple sources)	~ 4.0–3.7	3099	± 92.4	0.5	± 0.04	6190.2	± 573	1.9	± 0.3	0.38	± 0.03	5.1	± 0.8
Thaumasia Planum (20 pixels)	Volcanic Site	~ 3.8–3.7	2657	± 67.3	0.4	± 0.03	6581.5	± 588	2.0	± 0.2	0.41	± 0.03	4.9	± 0.6
Hesperia Planum (12 pixels)	Volcanic Site	~ 3.7	2655.5	± 81.5	0.44	± 0.04	6035.2	± 581	2.0	± 0.2	0.43	± 0.03	4.7	± 0.6
Apollinaris Mons (12 pixels)	Volcanic Site	~ 3.6–3.8	3331	± 104	0.63	± 0.05	5325	± 451	2.6	± 0.2	0.66	± 0.04	3.9	± 0.4
SCR (Arabia) (23 pixels)	Proposed Volcanic Site	~ 3.9–3.8	3990.8	± 117.6	0.74	± 0.05	5372	± 419	2.4	± 0.3	0.52	± 0.04	4.6	± 0.6
Broad SCR (Arabia) (48 pixels)	Larger region housing SCR	~ 3.9–3.8	3684	± 118.7	0.69	± 0.06	5336.7	± 460	2.3	± 0.2	0.49	± 0.03	4.7	± 0.6
Martian Crustal Proxy (1358 pixels)	(Excluding SCR and Broad SCR)		3523	± 100.7	0.61	± 0.05	5783.7	± 474	2.2	± 0.2	0.46	± 0.03	4.8	± 0.6

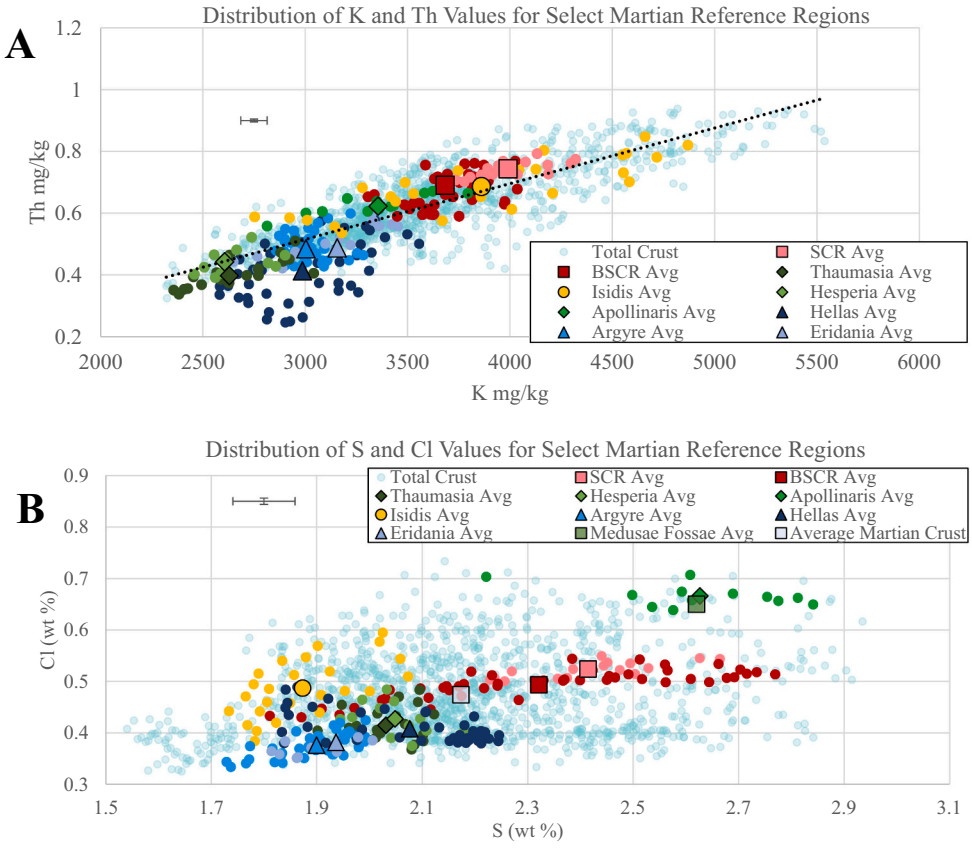

Fig. 2. (A) K and Th values for the entire crust (light blue), various color-coded regions and mean values (large polygons) with a linear trend fitted to the entire crust - as highlighted by the dotted line. SCR and BSCR are shown as squares, Isidis is represented by a circle, igneous references as diamonds and sedimentary references as triangles. Standard error for average values is displayed in top left of figure. Isidis, BSCR and SCR are grouped together at the higher end of observed K and Th abundances. SCR differs from Isidis in overall dispersion of K and Th abundances, with SCR having a much smaller dispersion in values. **(B)** Mean S and Cl values (formatting the same as in 2A), from chemical maps, along with the underlying data used to calculate the mean for reference regions on Mars, as well as S and Cl throughout the low to mid latitudes. MFF and Apollinaris Mons have the highest abundances of S and Cl, with SCR and BSCR reporting the second and third highest values, respectively. The remaining regions all have abundances lower than the crustal average. BSCR has a large dispersion in Cl values, much larger than what is observed for Apollinaris and SCR, both of which vary similarly. BSCR exhibits the largest range in values, whereas Apollinaris, Hellas, and SCR all show comparatively smaller range in S abundance. The remaining regions all exhibit abundances of S and Cl that are lower than the global average, and tend to cluster near each other, independent of provenance. (For interpretation of the references to color in this figure legend, the reader is referred to the web version of this article.)

et al., 2006), which may suggest that Thaumasia and Hesperia may have had some degree of secondary alteration after the end of their eruptive life. In an aqueous alteration environment, K is typically leached from minerals, leading to a low K/Th (Sawyer et al., 2000; Taylor et al., 2006). The fluid which is now enriched in K would inevitably flow into areas of low topography, the majority of which are craters on Mars. We observe that Hellas, Argyre and Eridania have high individual abundances of K and high K/Th in comparison to SCR and the average martian crust. It is likely the sedimentary materials in these basins became further enriched in K, and possibly Th, as fluids interacted with basaltic rocks and subsequently found their way into the topographic lows of these basins.

The mean values of S and Cl from Medusae Fossae (MFF) and Apollinaris Mons account for the highest observed values of both (Fig. 2B). Our Arabia regions show an intermediate abundance of S and Cl, compared to MFF, as well as the remaining sedimentary regions (Argyre, Hellas, Isidis, and Eridania) and volcanoes (Thaumasia and Hesperia planae). The high S and Cl abundance observed for the MFF and Apollinaris is attributed to millions of years of volcanic degassing and capture within the region (Diez et al., 2009; Ojha et al., 2019; Ojha et al., 2018). Since the MFF represents the accumulation of volcanic material over geologic timescales, its observed values for S and Cl suggest that volcanism is the only process that can enrich these two elements to such a high degree at a regional scale. The intermediate values of S and Cl found in SCR are also suggestive of enrichment through volcanic degassing. If the S and Cl abundances within SCR are from dust sourced from the MFF, they should fall within the global dust S/Cl range (3.0–4.4) which they do not (Table 1). This suggests that the S and Cl abundances within SCR are from local volcanism, which is capable of enriching material in these elements.

In addition to our geochemical analysis, we also performed an admittance analysis (see SI for analysis details), which can be used to determine properties of the crust such as densities and elastic thickness (Belleguic et al., 2005; Grott and Wieczorek, 2012; McGovern et al., 2002, 2004). Our admittance analysis over SCR reveals a load density that is consistent with porous, friable material, with the average density likely being lower than 2000 kg/m^3 (Fig. 3B). Additionally, we find that the elastic thickness in this region is equally low, likely not exceeding 20 km (Fig. 3C). This low elastic thickness suggests stronger mantle-lithosphere coupling and likely a high heat flow in the region. A higher heat flow, low elastic thickness and low load density are consistent with our hypothesis of volcanism within SCR.

4. Discussion

The shared enrichment in K and Th between Thaumasia and Hesperia Planae and our sedimentary references may suggest that these volcanoes have been subjected to aqueous alteration after the end of their eruptive life. However, since K is more soluble than Th, in order to for Thaumasia and Hesperia to have a high K/Th emplaced as a result of aqueous alteration, K-rich fluid must have been transported to each of these volcanoes and then accumulated to leave a K enrichment. This is physically unlikely, as each of these volcanoes are topographically high, and are composed primarily of geologic units attributed directly to their volcanic activity (Tanaka et al., 2014). Indeed, further investigation of Thaumasia Planum substantiates that the region's chemistry is not reflective of pervasive aqueous alteration (Hood et al., 2016).

It is equally likely that the observed K and Th abundances and K/Th within SCR (Fig. 2A) is suggestive of its volcanic provenance, not aqueous alteration. SCR's low dispersion in K and Th values, and K/Th

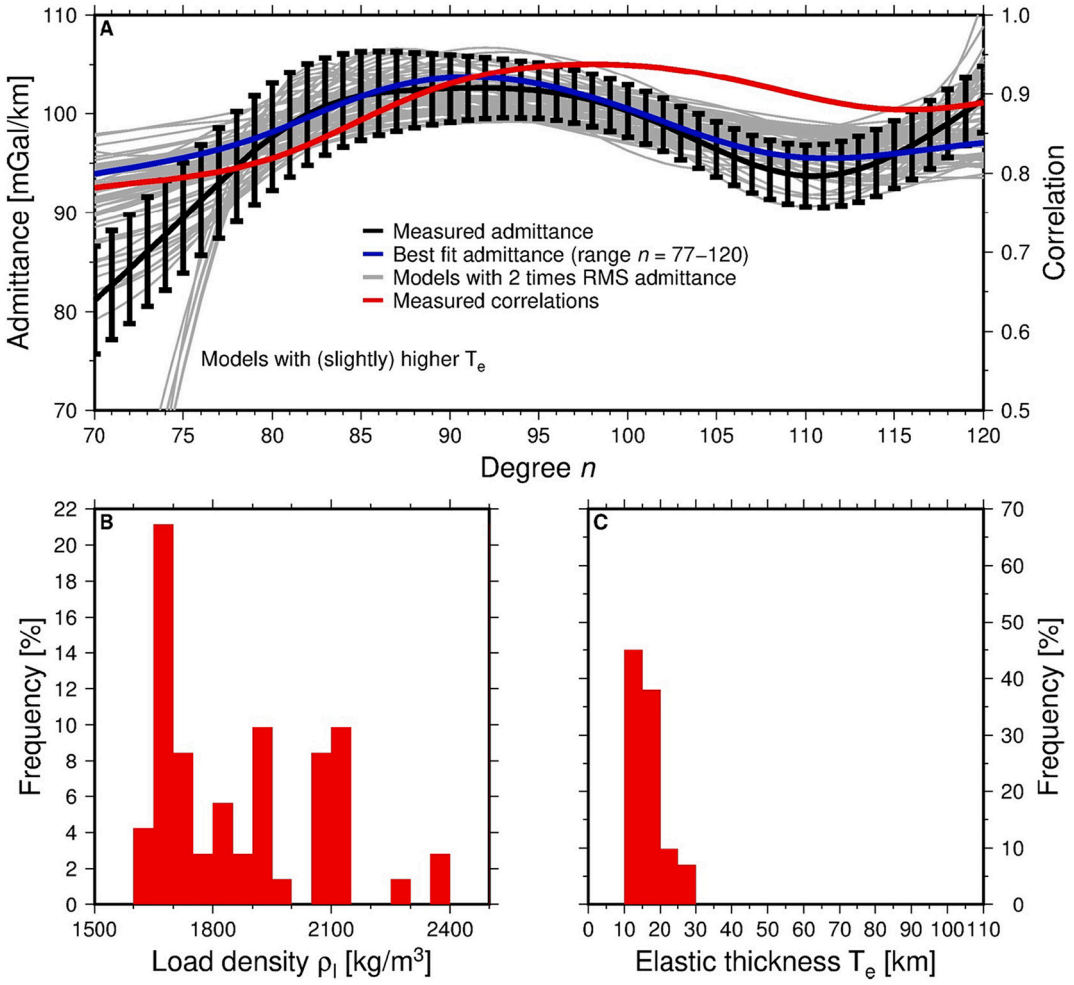

Fig. 3. Localized admittance and correlation between gravity and topography for the Arabia Terra area (centered on −5°E,25°N, for a spherical cap with a radius of 15°), including the best-fit theoretical admittance and models within two times this best fit (**A**). **A** shows the best-fit admittance model of our geophysical analyses, which has a root-mean-square (RMS) of the misfit between the theoretical model and measured admittance of 1.34 mGal/km for our windowed region (SI Appendix, Fig. S3) (degree range 77–120). The error bounds on the admittance shown in Fig. 3A are computed from the relationship between admittance variance and correlation (Wieczorek, 2008). Histograms of the values for load density (**B**) and elastic thickness (**C**) for the models are also included.

ratio which is similar to the crust, are all suggestive of primary igneous material that has not undergone aqueous alteration. There is also little evidence for a widespread presence of valley networks within SCR (Wordsworth et al., 2015), further evidence of limited aqueous alteration. In contrast, a high K/Th ratio is observed for Hellas, Eridania and Argyre (Table 1), consistent with regional aqueous alteration within the basins or accumulation of altered material therein (Taylor et al., 2006; Zalewska, 2013). SCR shows little chemical similarity to any of the sedimentary regions within the scope of this study (Fig. 2), suggesting that SCR's chemistry is unrelated to aqueous alteration. Furthermore, this also makes it unlikely that SCR's S abundances are related to sulfate deposits in aqueous (e.g., fluvial, playa, lacustrine) settings.

The S and Cl values within SCR reflect its volcanic provenance. S enrichment (Fig. 2B) supports an interpretation that sulfur is either adsorbed or chemically bound in the soil and regolith from volcanic degassing, because volcanic materials and gasses are rich in S (Bibring et al., 2006; Diez et al., 2009; Ojha et al., 2019). Furthermore, we can eliminate the possibility that dust, which is enriched in S and Cl (Berger et al., 2016), has made a significant contribution to SCR's S and Cl abundances. Martian dust has been shown to exhibit a constant molar ratio (Ojha et al., 2018) which is different from the S/Cl associated with volcanic degassing (Gaillard and Scaillet, 2009; King and McLennan, 2010; Ojha et al., 2019). Our calculated mean molar S/Cl ratio for SCR (~4.6) does not fall within the global dust molar ratio range (3.0–4.4) (Table 1; (Ojha et al., 2018). Additionally, Si and K abundances can provide additional corroboration, as dust mantled areas are generally depleted in these elements relative to the average crust (Berger et al., 2016; Lasue et al., 2018; Viviano et al., 2019). SCR is enriched in both Si and K (Supplementary Information, Fig. S2) compared to the crustal average, further discounting compositional contributions from dust mantling within SCR.

The combined indicators of unaltered igneous material within SCR, as well as S and Cl abundances inconsistent with martian dust suggest that SCR was resurfaced by volatile-rich, explosive volcanism. In order to significantly enrich S and Cl above average crustal values, volcanic degassing is required. The Medusae Fossae Formation (MFF) has the highest observed S and Cl values in this study (Fig. 2B), associated with its origin as a pyroclastic deposit from massive eruptions (Diez et al., 2009; Ojha and Lewis, 2018). This makes the MFF's S and Cl abundances key references for extensive explosive eruptions enhancing the volatile content of a region (Diez et al., 2009; Ojha et al., 2018). SCR is second in overall S and Cl abundances to Apollinaris (and by extension the MFF), which supports volcanic degassing as the primary mechanism which enhanced S and Cl within SCR (Diez et al., 2009; Ojha et al., 2018). It is unlikely that the observed S and Cl abundances are a result of localized weathering of bedrock, as this process is unlikely to substantially enrich S and Cl (Diez et al., 2009). This is best exhibited in our Eridania reference location, which contains portions of the Eridania Planitia,

located on the eastern rim of Hellas. Our Eridania reference exhibits one of the lowest overall abundances of S and Cl reported in this study (Fig. 2B) and is composed primarily of weathered volcanic material (Tanaka et al., 2014). Furthermore, the distinct S/Cl ratios between SCR and MFF suggest that the pyroclastic deposits that may constitute SCR's chemistry do not serve as a major source of martian dust.

The enrichment of H_2O along with S and Cl, given the rest of the chemical context of SCR, is further evidence of an explosive provenance. H_2O enrichment in volcanic tephras and glasses is commonplace, regardless of whether eruptions were derived from a volatile-rich magma or if the erupted material interacted with crustal volatiles prior to expulsion (Henderson et al., 2021). In addition, the mechanically weathered, fine-grained product from these glasses or tephras has been shown to hold significantly more water than smectites under martian surface pressure and temperature conditions (Jänchen et al., 2009). The observed H_2O enrichment likely represents some combination of volcanically derived H_2O-rich glasses or tephras and H_2O adsorption from their mechanically weathered products.

Geophysical modeling results also support the geochemical evidence for SCR's supereruptive provenance. We find a relatively low elastic thickness for SCR of ~15 km (Fig. 3C). This value is consistent with elastic thickness estimates within the Arabia region from earlier studies region (Belleguic et al., 2005; McGovern et al., 2004). Karimi et al. (2016; Fig. 8) and McGovern et al. (2004; Table 1), indicate a thermal gradient for Arabia exceeding 19 K/km and a heat flow between 47 and 75 mW/m^2, a range higher than for some martian volcanoes (McGovern et al., 2004). This estimate resembles prior heat flow estimates that report similar elastic thickness values within the Arabia.

Our geophysical analyses also yield a load density for SCR resembling the low densities for MFF (Ojha and Lewis, 2018) and that is consistent with thick pyroclastic deposits, formed through eruptions of buoyant magma containing dissolved gasses (McSween Jr., 1994). The regional load density as obtained from gravity and topography (Fig. 3; Supplementary Information, Fig. S3) is on average lower than 1900 kg/m^3. Our estimated load density also constrains the amount of degassed sulfur from eruptions. Using the minimum estimate for erupted volume (4600 km^3) for one patera within SCR (Michalski and Bleacher, 2013), and an average density of 1800 kg/m^3 (Fig. 3), we estimate a 8.3×10^8 kg maximum mass of erupted material. Of this total mass, approximately 2.0×10^7 kg is sulfur, based on our measured S abundances within SCR (average 2.4 wt% S; Table 1). If this mass represents the estimated 30% of the total S that may have been scavenged by ash, a percentage consistent with conservative estimates of atmospheric degassing (Ojha et al., 2019), the remaining mass of sulfur degassed to the atmosphere would be approximately 6.6×10^7 kg. Considering all four paterae with volumetrically equivalent concurrent eruptions, the amount of degassed sulfur increases to 2.6×10^8 kg. For comparison, the Toba eruption, the largest Quaternary volcanic eruption on Earth, emitted 10^{10}–10^{12} kg of sulfur (c.f. Ojha et al., 2018). If eruptions within SCR were brief and clustered temporally, such amounts of degassed sulfur alone would have impacted global climate (Halevy et al., 2007; Rampino and Self, 1992; Tian et al., 2010). These massive, climate-transforming, volatile and ash injections into the atmosphere would dramatically affect the stability and availability of water on the martian surface (Halevy et al., 2007; Tian et al., 2010). The possible onset of glaciation from ash expulsion and sulfur degassing (Halevy et al., 2007; Tian et al., 2010) within SCR would affect surface habitability, likely driving those habitable zones underground where it was warmer.

A multitude of processes could be responsible for influencing the melt composition prior to eruption, leading to the observed composition of the SCR. SCR exhibits enrichments not only in volatile species, but also in light elements, such as Si, Ca and Al (Supplementary Information, Fig. S2), the origin of which could be tied to primary melt composition. Enrichments in Ca and Si are expected, as Noachian primary melts are enriched in Ca and Si compared to younger melts (Baratoux et al., 2011, 2013). An enrichment in Al is difficult to explain through primary melt composition, as the martian mantle is largely believed to be depleted in Al (Mustard et al., 1997). We also observe an Fe enrichment in SCR, which could be a result of substantial crystallization as the magma evolved to produce a melt capable of explosive eruptions (Muir and Tilley, 1964). On Earth, this process generally favors enrichment of the major elements (Si, Al, Fe) within the melt at the expense of Mg content (Carmichael, 1964). Primary magmas are high in Mg and generally may increase in Fe and Ca during the first steps of fractional crystallization (Ostwald et al., 2022; Rapp et al., 2013). It is therefore possible that SCR's enrichments in Si, Fe, and Ca resulted from continued fractional crystallization, producing a more evolved melt which was eventually erupted. Typically, the amounts of fractional crystallization and crustal assimilation which are tied to magma residence time within a crustal reservoir correlate to eruptive explosivity (Reid, 2008). A low degree partial melt produced through prolonged residence time and continued fractional crystallization is a potential scenario which would result in explosive eruptions within SCR.

5. Conclusions

It is unlikely that SCR's chemistry has been influenced primarily by aqueous processes in the most recent past, as chemical evidence for aqueous alteration is lacking. K and Th are strongly coupled within SCR, where a decoupling would be expected if SCR was heavily affected by aqueous alteration. The K/Th ratio suggests that large floods interacting with local bedrock are unlikely, and individual Th abundance indicates low-pH alteration did not largely influence the chemistry of the SCR. In addition, it is unlikely that SCR functioned as a dust sink for much of its life due to chemical inconsistencies with other thickly mantled areas compared to the Martian crust (Supplementary Information, Fig. S1). It is therefore likely that the observed chemistry in SCR is from a past episode of volcanism, whose chemistry was unique among contemporaneous volcanoes. Our geophysical modeling results support an increased heat flow within SCR and a load density consistent with pyroclastic material, both of which are to be expected if explosive eruptions occurred.

The unique igneous chemistry within SCR is likely a result of SCR's supervolcanic provenance, where the magma could have (1) been sourced from a chemically distinct mantle or (2) spent significant time within a reservoir. It is difficult to discern which process dominated prior to eruptions within SCR. On Earth, the general trend among explosive eruptions is their infrequent occurrence (Reid, 2008), which is tied to the magma's residence time in a crustal reservoir (Solano et al., 2012). It is feasible that the same phenomenon occurs on Mars and may have assisted in increasing the explosivity of the eruptions within SCR. Indeed, the geochemical and geophysical evidence support a supereruptive provenance more so than either aqueous alteration or dust accumulation.

Funding

AB was funded by NASA-Mars Data Analysis Program grant 80NSSC18K1375 to SK, Louisiana NASA EPSCoR under cooperative agreement 80NSSC20M0150 (CFDA #43.008) to JML, and teaching assistantship in Geology & Geophysics at LSU. DRH, TP and SKN were also supported by 80NSSC18K1375.

Author contributions

AB, SK, SG designed research; AB, SG performed research; SK (deriving chemistry from gamma spectra) and JML (geophysics) guided the data analysis and interpretations also as the dissertation advisors; DRH contributed to reference region selection, LO to geophysical interpretations, TP and SKN on volcanic eruptions. AB, SG analyzed data; AB wrote the manuscript with participation by all co-authors.

Data and materials availability

Mapped geology for Mars was acquired from the USGS archive (https://pubs.usgs.gov/sim/3292/) developed by Tanaka et al. (2014) and subsequent analysis of this data was performed using ArcGIS software. GRS spectra are from the NASA Planetary Database System (PDS, https://pds-geosciences.wustl.edu/missions/odyssey/grs_cgs.html). Topographic data are from the Mars Orbiter Laser Altimeter (MOLA) data, also archived at NASA PDS, and used in the MarsTopo2600 model (Wieczorek, 2015), see https://figshare.com/articles/dataset/Spherical_harmonic_model_of_the_shape_of_Mars_MarsTopo2600/12402653). The gravity model used in our analysis can be found at the NASA/GSFC PGDA website (https://pgda.gsfc.nasa.gov/products/63). Details of data sources follow in their respective sections.

Declaration of Competing Interest

Authors declare that they have no competing interests.

Data availability

Data will be made available on request.

Acknowledgments

Dr. Joe Levy provided topical advice on the manuscript. We would also like to thank Dr. Brian Balta and our anonymous reviewer for their incisive comments and revisions.

Appendix A. Supplementary data

Supplementary data to this article can be found online at https://doi.org/10.1016/j.icarus.2022.115303.

References

Albarede, F., 2009. Geochemistry: An Introduction, 2nd ed. Cambridge University Press.
Baines, P.G., Sparks, R.S.J., 2005. Dynamics of giant volcanic ash clouds from supervolcanic eruptions. Geophys. Res. Lett. 32, 1–4. https://doi.org/10.1029/2005GL024597.
Bandfield, J.L., Edwards, C.S., Montgomery, D.R., Brand, B.D., 2013. The dual nature of the martian crust: young lavas and old clastic materials. Icarus 222, 188–199. https://doi.org/10.1016/j.icarus.2012.10.023.
Baratoux, D., Toplis, M.J., Monnereau, M., Gasnault, O., 2011. Thermal history of Mars inferred from orbital geochemistry of volcanic provinces. Nature 472, 338–341. https://doi.org/10.1038/nature09903.
Baratoux, D., Toplis, M.J., Monnereau, M., Sautter, V., 2013. The petrological expression of early Mars volcanism. J. Geophys. Res. E Planets 118, 59–64. https://doi.org/10.1029/2012JE004234.
Baratoux, D., Samuel, H., Michaut, C., Toplis, M.J., Monnereau, M., Wieczorek, M., Garcia, R., Kurita, K., 2014. Petrological constraints on the density of the Martian crust. J. Geophys. Res. 119, 1707–1727. https://doi.org/10.1002/2014JE004642.
Belleguic, V., Lognonné, P., Wieczorek, M., 2005. Constraints on the Martian lithosphere from gravity and topography data. J. Geophys. Res. E Planets 110, 1–22. https://doi.org/10.1029/2005JE002437.
Berger, J.A., Schmidt, M.E., Gellert, R., Campbell, J.L., King, P.L., Flemming, R.L., Ming, D.W., Clark, B.C., Pradler, I., Vanbommel, S.J.V., Minitti, M.E., Fairén, A.G., Boyd, N.I., Thompson, L.M., Perrett, G.M., Elliott, B.E., Desouza, E., 2016. A global Mars dust composition refined by the alpha-particle X-ray spectrometer in Gale crater. Geophys. Res. Lett. 43, 67–75. https://doi.org/10.1002/2015GL066675.
Bibring, J.-P., Langevin, Y., Mustard, J.F., Poulet, F., Arvidson, Raymond, Gendrin, A., Gondet, B., Mangold, N., Pinet, P., Forget, F., Berthé, M., Bibring, J.-P., Gendrin, A., Gomez, C., Gondet, B., Jouglet, D., Poulet, F., Soufflot, A., Vincendon, M., Combes, M., Drossart, P., Encrenaz, T., Fouchet, T., Merchiorri, R., Belluci, G., Altieri, F., Formisano, V., Capaccioni, F., Cerroni, P., Coradini, A., Fonti, S., Korablev, O., Kottsov, V., Ignatiev, N., Moroz, V., Titov, D., Zasova, L., Loiseau, D., Mangold, N., Pinet, Patrick, Douté, S., Schmitt, B., Sotin, C., Hauber, E., Hoffmann, H., Jaumann, R., Keller, U., Arvidson, Ray, Mustard, J.F., Duxbury, T., Forget, François, Neukum, G., 2006. Global mineralogical and aqueous mars history derived from OMEGA/Mars express data. Science 312, 400–404. https://doi.org/10.1126/science.1122659.
Boynton, W.V., Taylor, G.J., Evans, L.G., Reedy, R.C., Starr, R., Janes, D.M., Kerry, K.E., Drake, D.M., Kim, K.J., Williams, R.M.S., Crombie, M.K., Dohm, J.M., Baker, V., Metzger, A.E., Karunatillake, S., Keller, J.M., Newsom, H.E., Arnold, J.R., Brückner, J., Englert, P.A.J., Gasnault, O., Sprague, A.L., Mitrofanov, I., Squyres, S. W., Trombka, J.I., D'Uston, L., Wänke, H., Hamara, D.K., 2007. Concentration of H, Si, Cl, K, Fe, and Th in the low- and mid-latitude regions of Mars. J. Geophys. Res. 112, E12S99 https://doi.org/10.1029/2007JE002887.
Burton, M.R., Caltabiano, T., Murè, F., Salerno, G., Randazzo, D., 2009. SO2 flux from Stromboli during the 2007 eruption: results from the FLAME network and traverse measurements. J. Volcanol. Geotherm. Res. 182, 214–220. https://doi.org/10.1016/j.jvolgeores.2008.11.025.
Carmichael, I.S.E., 1964. The petrology of thingmuli, a tertiary volcano in eastern Iceland. J. Petrol. 5, 435–460. https://doi.org/10.1093/petrology/5.3.435.
Carnes, L.L., Karunatillake, S., Susko, D.A., Hood, D.R., 2017. Delineating the Arabia Terra region on Mars to investigate paterae orgins. In: LPSC2017. https://doi.org/10.1038/ngeo2845. Abstract 1756.
Diez, B., Feldman, W.C., Mangold, N., Baratoux, D., Maurice, S., Gasnault, O., D'Uston, L., Costard, F., 2009. Contribution of Mars odyssey GRS at central Elysium Planitia. Icarus 200, 19–29. https://doi.org/10.1016/j.icarus.2008.11.011.
Dohm, J.M., Barlow, N.G., Anderson, R.C., Williams, J.-P., Miyamoto, H., Ferris, J.C., Strom, R.G., Taylor, G.J., Fairén, A.G., Baker, V.R., Boynton, W.V., Keller, J.M., Kerry, K.E., Janes, D.M., Rodriguez, J.A.P., Hare, T.M., 2007. Possible ancient giant basin and related water enrichment in the Arabia Terra province, Mars. Icarus 190, 74–92. https://doi.org/10.1016/j.icarus.2007.03.006.
Edmonds, M., Wallace, P.J., 2017. Volatiles and exsolved vapor in volcanic systems. Elements 13, 29–34. https://doi.org/10.2113/gselements.13.1.29.
Ehlmann, B.L., Mustard, J.F., Murchie, S.L., Bibring, J.-P., Meunier, A., Fraeman, A.A., Langevin, Y., 2011. Subsurface water and clay mineral formation during the early history of Mars. Nature 479, 53–60. https://doi.org/10.1038/nature10582.
Gaillard, F., Scaillet, B., 2009. The sulfur content of volcanic gases on Mars. Earth Planet. Sci. Lett. 279, 34–43. https://doi.org/10.1016/j.epsl.2008.12.028.
Goossens, S., Sabaka, T.J., Genova, A., Mazarico, E., Nicholas, J.B., Neumann, G.A., 2017. Evidence for a low bulk crustal density for Mars from gravity and topography. Geophys. Res. Lett. 1–9 https://doi.org/10.1002/2017GL074172.
Grott, M., Wieczorek, M.A., 2012. Density and lithospheric structure at Tyrrhena Patera, Mars, from gravity and topography data. Icarus 221, 43–52. https://doi.org/10.1016/j.icarus.2012.07.008.
Halevy, I., Zuber, M.T., Schrag, D.P., 2007. A sulfur dioxide climate feedback on early Mars. Science 318, 1903–1908. https://doi.org/10.5040/9780755621101.0007.
Henderson, M.J.B., Horgan, B.H.N., Rowe, M.C., Wall, K.T., Scudder, N.A., 2021. Determining the volcanic eruption style of tephra deposits from infrared spectroscopy. Earth Space Sci. 8 https://doi.org/10.1029/2019EA001013.
Hood, D.R., Judice, T., Karunatillake, S., Rogers, D., Dohm, J.M., Susko, D.A., Carnes, L. K., 2016. Assessing the geologic evolution of greater Thaumasia, Mars. J. Geophys. Res. Planets 121, 1753–1769. https://doi.org/10.1002/2016JE005046.
Jänchen, J., Morris, R.V., Bish, D.L., Janssen, M., Hellwig, U., 2009. The H2O and CO2 adsorption properties of phyllosilicate-poor palagonitic dust and smectites under martian environmental conditions. Icarus 200, 463–467. https://doi.org/10.1016/j.icarus.2008.12.006.
Karimi, Saman, Dombard, Andrew J., Buczkowski, Debra L., Robbins, Stuart J., Williams, Rebecca M., 2016. Using the viscoelastic relaxation of large impact craters to study the thermal history of Mars. Icarus 272, 102–113. https://doi.org/10.1016/j.icarus.2016.02.037.
Karunatillake, S., Squyres, S.W., Taylor, G.J., Keller, J.M., Gasnault, O., Evans, L.G., Reedy, R.C., Starr, R., Boynton, W.V., Janes, D.M., Kerry, K.E., Dohm, J.M., Sprague, A.L., Hahn, B.C., Hamara, D., 2006. Composition of northern low-albedo regions of Mars: insights from the Mars odyssey gamma ray spectrometer. J. Geophys. Res. 111, E03S05. https://doi.org/10.1029/2006JE002675.
Karunatillake, S., Wray, J.J., Squyres, S.W., Taylor, G.J., Gasnault, O., McLennan, S.M., Boynton, W., El-Maarry, M.R., Dohm, J.M., 2009. Chemically striking regions on Mars and stealth revisited. J. Geophys. Res. 114, E12001. https://doi.org/10.1029/2008JE003303.
Keller, J.M., Boynton, W.V., Karunatillake, S., Baker, V.R., Dohm, J.M., Evans, L.G., Finch, M.J., Hahn, B.C., Hamara, D.K., Janes, D.M., Kerry, K.E., Newsom, H.E., Reedy, R.C., Sprague, A.L., Squyres, S.W., Starr, R.D., Taylor, G.J., Williams, R.M.S., 2006. Equatorial and midlatitude distribution of chlorine measured by Mars odyssey GRS. J. Geophys. Res. 112, E03S08. https://doi.org/10.1029/2006JE002679.
Kerber, L., Head, J.W., 2010. The age of the Medusae fossae formation: evidence of Hesperian emplacement from crater morphology, stratigraphy, and ancient lava contacts. Icarus 206, 669–684. https://doi.org/10.1016/j.icarus.2009.10.001.
Kerber, L., Head, J.W., Madeleine, J.-B., Forget, F., Wilson, L., 2012. The dispersal of pyroclasts from ancient explosive volcanoes on Mars: implications for the friable layered deposits. Icarus 219, 358–381. https://doi.org/10.1016/j.icarus.2012.03.016.
King, P.L., McLennan, S.M., 2010. Sulfur on Mars. Elements 6, 107–112. https://doi.org/10.2113/gselements.6.2.107.
Lasue, J., Cousin, A., Meslin, P.Y., Mangold, N., Wiens, R.C., Berger, G., Dehouck, E., Forni, O., Goetz, W., Gasnault, O., Rapin, W., Schroeder, S., Ollila, A., Johnson, J., Le Mouélic, S., Maurice, S., Anderson, R., Blaney, D., Clark, B., Clegg, S.M., d'Uston, C., Fabre, C., Lanza, N., Madsen, M.B., Martin-Torres, J., Melikechi, N., Newsom, H., Sautter, V., Zorzano, M.P., 2018. Martian Eolian dust probed by ChemCam. Geophys. Res. Lett. 45, 10,968–10,977. https://doi.org/10.1029/2018GL079210.
McGovern, P.J., Solomon, S.C., Smith, D.E., Zuber, M.T., Simons, M., Wieczorek, M.A., Phillips, R.J., Neumann, G.A., Aharonson, O., Head, J.W., 2002. Localized gravity/topography admittance and correlation spectra on Mars: implications for regional and global evolution. J. Geophys. Res. Planets 107. https://doi.org/10.1029/2002JE001854, 19-1-19-25.
McGovern, P.J., Solomon, S.C., Smith, D.E., Zuber, M.T., Simons, M., Wieczorek, M.A., Phillips, R.J., Neumann, G.A., Aharonson, O., Head, J.W., 2004. Correction to "Localized gravity/topography admittance and correlation spectra on Mars:

Implications for regional and global evolution". J. Geophys. Res. E Planets 109. https://doi.org/10.1029/2002je001854, 19–1.
McSween Jr., H.Y., 1994. What we have learned about Mars from SNC meteorites. Meteoritics 29, 757–779.
Michalski, J.R., Bleacher, J.E., 2013. Supervolcanoes within an ancient volcanic province in Arabia Terra, Mars. Nature 502, 47–52. https://doi.org/10.1038/nature12482.
Muir, I.D., Tilley, C.E., 1964. Iron enrichment and pyroxene fractionation in tholeiites. Geol. J. 4, 143–156. https://doi.org/10.1002/gj.3350040111.
Mustard, J.F., Murchie, S., Erard, S., Sunshine, J., 1997. In situ compositions of Martian volcanics: implications for the mantle. J. Geophys. Res. 102, 25605. https://doi.org/10.1029/97JE02354.
Newsom, H.E., Crumpler, L.S., Reedy, R.C., Petersen, M.T., Newsom, G.C., Evans, L.G., Taylor, G.J., Keller, J.M., Janes, D.M., Boynton, W.V., Kerry, K.E., Karunatillake, S., 2007. Geochemistry of Martian soil and bedrock in mantled and less mantled terrains with gamma ray data from Mars odyssey. J. Geophys. Res. 112, E03S12. https://doi.org/10.1029/2006JE002680.
Ojha, L., Lewis, K., 2018. The density of the Medusae fossae formation: implications for its composition, origin, and importance in Martian history. J. Geophys. Res. Planets 123, 1368–1379. https://doi.org/10.1029/2018JE005565.
Ojha, L., Lewis, K., Karunatillake, S., Schmidt, M., 2018. The Medusae fossae formation as the single largest source of dust on Mars. Nat. Commun. 9, 1–7. https://doi.org/10.1038/s41467-018-05291-5.
Ojha, L., Karunatillake, S., Lacovino, K., 2019. Atmospheric injection of sulfur from the Medusae fossae forming events. Planet. Space Sci. 179, 104734 https://doi.org/10.1016/j.pss.2019.104734.
Ostwald, A., Udry, A., Payré, V., Gazel, E., Wu, P., 2022. The role of assimilation and fractional crystallization in the evolution of the Mars crust. Earth Planet. Sci. Lett. 585, 117514 https://doi.org/10.1016/j.epsl.2022.117514.
Rampino, M.R., Self, S., 1992. Volcanic winter and accelerated glaciation following the Toba super-eruption. Nature 359, 50–52. https://doi.org/10.1038/359050a0.
Rapp, J.F., Draper, D.S., Mercer, C.M., 2013. Anhydrous liquid line of descent of Yamato-980459 and evolution of Martian parental magmas. Meteorit. Planet. Sci. 48, 1780–1799. https://doi.org/10.1111/maps.12197.
Reid, M.R., 2008. How long does it take to supersize an eruption. Elements 4, 23–28. https://doi.org/10.2113/GSELEMENTS.4.1.23.
Robbins, S.J., Di Achille, G., Hynek, B.M., 2011. The volcanic history of Mars: high-resolution crater-based studies of the calderas of 20 volcanoes. Icarus 211, 1179–1203. https://doi.org/10.1016/j.icarus.2010.11.012.
Sawyer, D.J., McGehee, M.D., Canepa, J., Moore, C.B., 2000. Water soluble ions in the Nakhla martian meteorite. Meteorit. Planet. Sci. 35, 743–747. https://doi.org/10.1111/j.1945-5100.2000.tb01458.x.
Solano, J.M.S., Jackson, M.D., Sparks, R.S.J., Blundy, J.D., Annen, C., 2012. Melt segregation in deep crustal hot zones: a mechanism for chemical differentiation, crustal assimilation and the formation of evolved magmas. J. Petrol. 53, 1999–2026. https://doi.org/10.1093/petrology/egs041.
Spilliaert, N., Allard, P., Métrich, N., Sobolev, A.V., 2006. Melt inclusion record of the conditions of ascent, degassing, and extrusion of volatile-rich alkali basalt during the powerful 2002 flank eruption of Mount Etna (Italy). J. Geophys. Res. Solid Earth 111. https://doi.org/10.1029/2005JB003934.
Tanaka, K.L., 2000. Dust and ice deposition in the Martian geologic record. Icarus 144, 254–266. https://doi.org/10.1006/icar.1999.6297.
Tanaka, K.L., Robbins, S.J., Fortezzo, C.M., Skinner, J.A., Hare, T.M., 2014. The digital global geologic map of Mars: chronostratigraphic ages, topographic and crater morphologic characteristics, and updated resurfacing history. Planet. Space Sci. 95, 11–24. https://doi.org/10.1016/j.pss.2013.03.006.
Taylor, G.J., Stopar, J.D., Boynton, W.V., Karunatillake, S., Keller, J.M., Brückner, J., Wänke, H., Dreibus, G., Kerry, K.E., Reedy, R.C., Evans, L.G., Starr, R.D., Martel, L.M. V., Squyres, S.W., Gasnault, O., Maurice, S., D'Uston, C., Englert, P., Dohm, J.M., Baker, V.R., Hamara, D.K., Janes, D.M., Sprague, A.L., Kim, K.J., Drake, D.M., McLennan, S.M., Hahn, B.C., 2006. Variations in K/Th on mars. J. Geophys. Res. 112, E03S06. https://doi.org/10.1029/2006JE002676.
Taylor, G.J., Martel, L.M.V., Karunatillake, S., Gasnault, O., Boynton, W.V., 2010. Mapping mars geochemically. Geology 38, 183–186. https://doi.org/10.1130/G30470.1.
Tian, F., Claire, M.W., Haqq-Misra, J.D., Smith, M., Crisp, D.C., Catling, D., Zahnle, K., Kasting, J.F., 2010. Photochemical and climate consequences of sulfur outgassing on early Mars. Earth Planet. Sci. Lett. 295, 412–418. https://doi.org/10.1016/j.epsl.2010.04.016.
Viviano, C., Murchie, S.L., Daubar, I.J., Morgan, M.F., Seelos, F.P., Plescia, J.B., 2019. Composition of Amazonian volcanic materials in Tharsis and Elysium, Mars, from MRO/CRISM reflectance spectra. Icarus 328, 274–286. https://doi.org/10.1016/j.icarus.2019.03.001.
Whelley, P., Matiella Novak, A., Richardson, J., Bleacher, J., Mach, K., Smith, R.N., 2021. Stratigraphic evidence for early Martian explosive volcanism in Arabia Terra. Geophys. Res. Lett. 48, 1–12. https://doi.org/10.1029/2021GL094109.
Wieczorek, M.A., 2008. Constraints on the composition of the martian south polar cap from gravity and topography. Icarus 196, 506–517. https://doi.org/10.1016/j.icarus.2007.10.026.
Wieczorek, M.A., 2015. Gravity and Topography of the Terrestrial Planets. Treatise on Geophysics 10, 153–193. https://doi.org/10.1016/B978-0-444-53802-4.00169-X.
Wieczorek, M.A., Broquet, A., McLennan, S.M., Rivoldini, A., Golombek, M., Antonangeli, D., Beghein, C., Giardini, D., Gudkova, T., Gyalay, S., Johnson, C.L., Joshi, R., Kim, D., King, S.D., Knapmeyer-Endrun, B., Lognonné, P., Michaut, C., Mittelholz, A., Nimmo, F., Ojha, L., Panning, M.P., Plesa, A., Siegler, M.A., Smrekar, S.E., Spohn, T., Banerdt, W.B., 2022. InSight constraints on the global character of the Martian crust. J. Geophys. Res. Planets 127, 1–35. https://doi.org/10.1029/2022je007298.
Wordsworth, R.D., Kerber, L., Pierrehumbert, R.T., Forget, F., Head, J.W., 2015. Comparison of "warm and wet" and "cold and icy" scenarios for early Mars in a 3D climate model. J. Geophys. Res. Planets. https://doi.org/10.1002/2015JE004787.
Zalewska, N., 2013. Hellas Planitia as a potential site of sedimentary minerals. Planet. Space Sci. 78, 25–32. https://doi.org/10.1016/j.pss.2012.12.006.